

The Low- α Splash Population in the Milky Way

LAIS BORBOLATO ¹, JOÃO A. S. AMARANTE ^{2,3}, HÉLIO D. PEROTTONI ⁴, SILVIA ROSSI ¹,
VICTOR P. DEBATTISTA ⁵, ZHAO-YU LI ^{2,3}, NATHAN DEG ⁶ AND TIGRAN KHACHATURYANTS ^{2,3}

¹Universidade de São Paulo, Instituto de Astronomia, Geofísica e Ciências Atmosféricas, Departamento de Astronomia, SP 05508-090, São Paulo, Brasil

²Department of Astronomy, School of Physics and Astronomy,

Shanghai Jiao Tong University, 800 Dongchuan Road, Shanghai, 200240, China

³State Key Laboratory of Dark Matter Physics, School of Physics and Astronomy, Shanghai Jiao Tong University, Shanghai, 200240, China

⁴Observatório Nacional, MCTI, Rua Gal. José Cristino 77, Rio de Janeiro, 20921-400, RJ, Brazil

⁵Jeremiah Horrocks Institute, University of Lancashire, Preston, PR1 2HE, UK

⁶Department of Physics, Engineering Physics, and Astronomy, Queen's University, Kingston ON K7L 3N6, Canada

ABSTRACT

The Milky Way in-situ halo, also known as the Splash, consists of old (Age > 10 Gyr), metal-rich ([Fe/H] > -0.7), high- α stars, i.e. thick disk-like chemistry, on halo-like orbits (eccentricity > 0.6). Its origin is linked to stars formed in the disk and dynamically heated by either internal or external agents. In this work, we investigate its low- α counterpart, the *low- α Splash*, motivated by recent findings of an old thin disk population. We conjecture that any mechanism capable of heating disk stars should affect both of present-day high- and low- α old populations. Using data from the APOGEE DR17 spectroscopic catalog, we identify metal-rich low- α stars with halo-like kinematics similar to those of the classical high- α Splash. We investigate their possible heating mechanisms using GASTRO suite of simulations, which allow us to explore the effects of star-forming clumps as well as a major merger in the proto-disk of a Milky Way analog galaxy. Our main results show that only clumpy Milky Way models are able to produce Splash populations through scattering by clumps in the early Galaxy, including the low- α counterpart, whereas the model including only the merger and without an early clumpy phase fails to produce these populations. In the models, the low- α Splash corresponds to a subset of the old thin disk that was dynamically heated by the same mechanism responsible for the formation of the high- α Splash.

Keywords: Galaxy: disk - Galaxy: structure - stars: abundance - stars: dynamical

1. INTRODUCTION

The mechanisms driving the formation and evolution of the Milky Way (MW) over the past 13 billion years continue to be extensively investigated in the field of Galactic Archaeology (e.g., Freeman & Bland-Hawthorn 2002; Bland-Hawthorn & Gerhard 2016; Barbuy et al. 2018; Helmi 2020). A key approach involves studying the chemodynamical properties of the halo, bulge, and disk, focusing on populations that retain signatures of major evolutionary events, such as the dynamically heated disk population. Initially identified as metal-rich halo stars ([Fe/H] > -1.0; Sheffield et al. 2012; Hawkins et al. 2015b), these objects were interpreted as stars ejected from the Galactic disk. The advent of the

Gaia era (Gaia Collaboration et al. 2016) and large spectroscopic surveys enabled the identification of hundreds of similar stars, and characterized these as an old, high- α population (e.g., Bonaca et al. 2017; Di Matteo et al. 2019; Gallart et al. 2019; Belokurov et al. 2020; Bonaca et al. 2020), consistent with a dynamically heated early disk.

Several works have sought to understand the formation of this population, leading to the prevailing interpretation that these stars were born in the early MW disk and then dynamically heated by the last major merger with the dwarf galaxy Gaia-Sausage/Enceladus (GSE; Belokurov et al. 2018; Haywood et al. 2018; Helmi et al. 2018), 9–11 Gyr ago (Gallart et al. 2019; Montalbán et al. 2021). This population was dubbed “Splash” by Belokurov et al. (2020), in reference to its likely formation pathway through a massive merger (e.g. Grand et al. 2020; Liao et al. 2024; Orkney & Laporte 2025). Contrary to this main interpretation, several mecha-

Corresponding author: Lais Borbolato (laisborbolato@usp.br), João A. S. Amarante (joaoant@gmail.com)

nisms have been suggested for the formation of the Splash: i) scattering by massive star-forming clumps in early disk galaxies without the need for a merger event (Amarante et al. 2020a); ii) scattering by minor mergers (Dillamore et al. 2022; Kisku et al. 2025), and iii) an origin tied to the dispersion-dominated nature of the proto-galaxy (Buder et al. 2025).

Historically, the high- α /thick¹ and low- α /thin disks have been interpreted as a sequential formation process (e.g., Chiappini et al. 1997; Grisoni et al. 2017), where the thick disk formed first and the thin disk later, after dilution of the star-forming gas by accretion events such as major mergers (e.g., Spitoni et al. 2019) or cosmic filaments (Agertz et al. 2021; Renaud et al. 2021). However, recent observations suggest that the early disk was not composed solely of a high- α population, but that low- α stars co-formed with the high- α disk during the first billion years of the MW (Silva Aguirre et al. 2018; Beraldo e Silva et al. 2021; Nepal et al. 2024; Gent et al. 2024; Borbolato et al. 2025). Borbolato et al. (2025) showed that low- α stars predate the GSE merger, which leads us to conjecture that the same dynamical heating mechanism responsible for the high- α Splash should also have impacted the old low- α disk, potentially forming a low- α counterpart to the Splash. While recent studies report low- α stars on halo-like orbits (Ortigoza-Urdaneta et al. 2023; Nepal et al. 2024; Filion et al. 2025), their origin remains debated, and its direct association with the high- α Splash population has not yet been established.

Until now, two models have been proposed to explain the formation of the ancient thin disk component ($z \sim 2$). One is the revised parallel model presented by Grisoni et al. (2026), while the other is the clumpy model (Beraldo e Silva et al. 2020; Amarante et al. 2025). The latter also reproduces the chemo-geometric thin and thick disks (Clarke et al. 2019; Beraldo e Silva et al. 2020), and the chemistry of the bulge (Debattista et al. 2023). The possibility that the MW may have hosted clumps is also highly motivated by observations of clumpy galaxies (e.g., Bournaud et al. 2008; Puech 2010; Guo et al. 2015; Zanella et al. 2019; Adams et al. 2025; Sok et al. 2025), with a peak around redshift $z \sim 2$ (e.g., Shibuya et al. 2016; Sattari et al. 2023; de la Vega et al. 2025), and the identification of galaxies analogous to MW progenitors hosting clumps (Tan et al. 2025). Also, da Silva & Smiljanic (2025) report that one very metal-poor r-process enriched star may be formed in a clump present in the early Galaxy. The clumpy model has proven to be a mechanism that likely played an important role in the formation of the MW disk and should therefore be considered in our investigation.

In this Letter, we demonstrate the existence of a low- α Splash population. We compare it with the canonical

high- α Splash and explore possible formation pathways using the Gaia–EncelAdus–Sausage Timing, chemistRy and Orbit (GASTRO; Amarante et al. 2022, 2025) simulations, examining the effects of star-forming clumps and a GSE-like merger on a MW-like disk. This Letter is organized as follows: Section 2 presents the observational and simulated data. Section 3 presents the results found, and they are discussed in Section 4. Finally, Section 5 summarizes our main conclusions.

2. DATA

2.1. Observacional data

We use data from the Apache Point Observatory Galactic Evolution Experiment (APOGEE; Majewski et al. 2017) Data Release 17 (DR17; Abdurro’uf et al. 2022) spectroscopic survey, utilizing its high resolution ($R \sim 22,000$) near-infrared spectrograph (Wilson et al. 2019) and H -band ($1.51\mu\text{m}$ – $1.69\mu\text{m}$) coverage to distinguish the MW disk’s high- and low- α populations (Imig et al. 2023).

Astrometric parameters are obtained from *Gaia DR3* (Gaia Collaboration et al. 2023), with distances derived via the spectro-photometric StarHorse Bayesian code (Queiroz et al. 2023). Orbital integrations are performed for 20 Gyr forward using the AGAMA library (Vasiliev 2019), adopting the Galactic potential model of McMillan (2017). We assume the Sun’s position with respect to the Galactic Center to be $(X, Y, Z)_{\text{GC}} = (-8.2, 0.0, 0.0)$ kpc (Bland-Hawthorn & Gerhard 2016), with the local circular velocity $v_{\text{circ}} = 232.8 \text{ km s}^{-1}$ (McMillan 2017), and the solar motion relative to the local standard of rest of $(U_{\odot}, V_{\odot}, W_{\odot}) = (11.10, 12.24, 7.25) \text{ km s}^{-1}$ (Schönrich et al. 2010). Here, we consider that positive azimuthal velocity ($V_{\phi} > 0 \text{ km s}^{-1}$) corresponds to the sense of rotation of the disk.

Our sample consists of red giants ($4000 < T_{\text{eff}}(\text{K}) < 6500$, $\log g < 3$) with a good signal-to-noise ratio ($S/N > 50$) and sources with no spectral or parameter issues (STARFLAG == 0, Jönsson et al. 2020). We require unflagged abundances for [Fe/H], [Mg/Fe], [Mg/Mn], and [Al/Fe] (i.e., flagged == 0). We adopt the recommended cut on the renormalized unit weight error (RUWE ≤ 1.4 ; Lindgren et al. 2021), a fractional distance uncertainty of $d/\sigma_d > 5$ and `parallax_over_error` > 5 . After applying these quality cuts, the APOGEE sample contains 108,911 stars

2.2. MW-analogues with GASTRO Library

We use a subset of the GASTRO (Amarante et al. 2022, 2025) library suite of simulations to explore the formation of the low- α Splash population. GASTRO consists of N-body + smoothed particle hydrodynamics (SPH) simulations designed to investigate the impact of a single merger-event aimed at reproducing a GSE analog, as well as the role of high-star-formation clumps on the structure and evolution of an MW-like galaxy. We

¹ Here, we use low- α (high- α) disk as a synonym for the chemical thin (thick) disk.

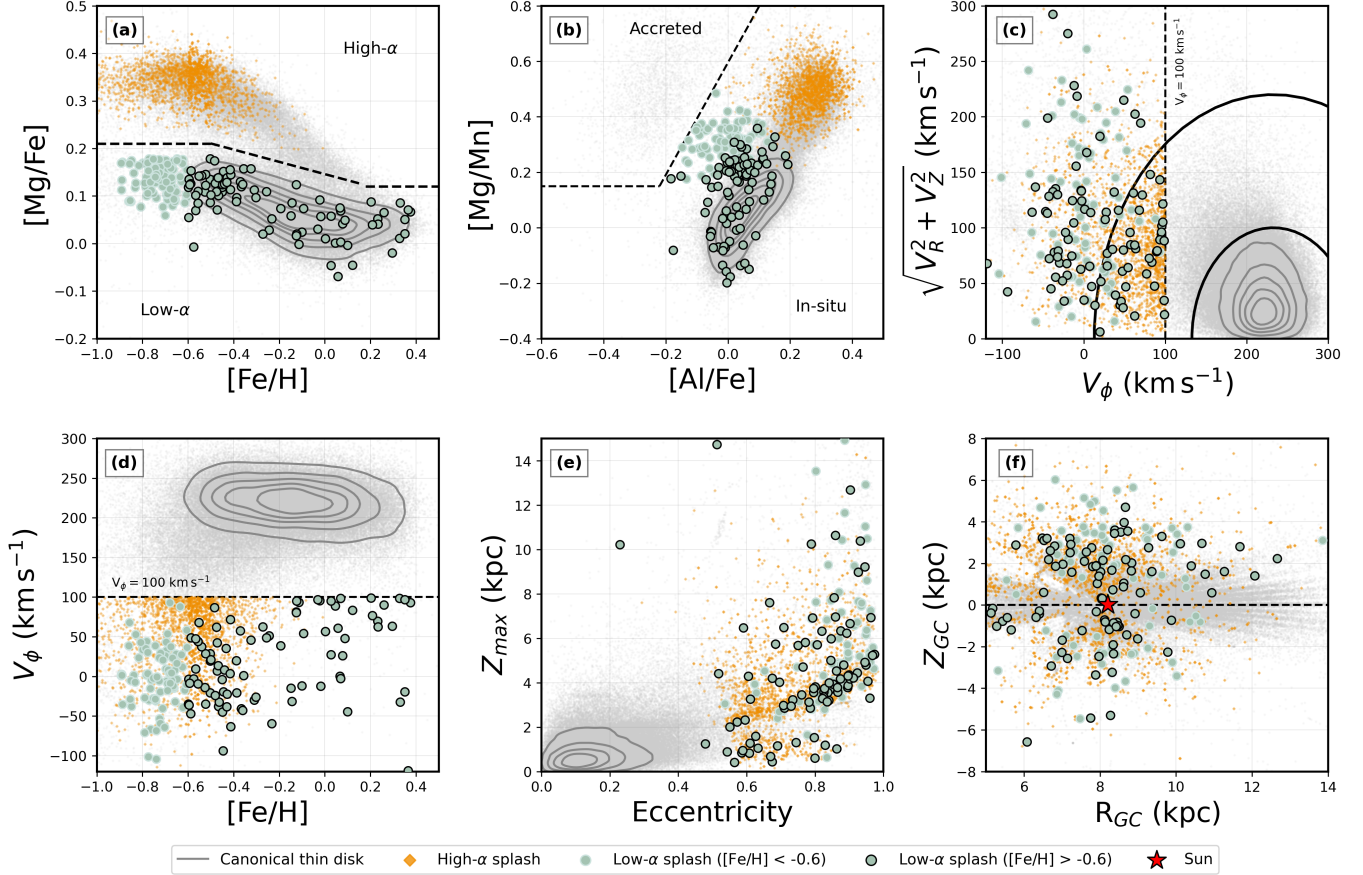


Figure 1. Projection of the Low- α Splash (green dots) and High- α Splash (orange points) in the (a) $[\text{Mg}/\text{Fe}]$ – $[\text{Fe}/\text{H}]$, where the dotted line indicates the separation between high- and low- α regions; (b) $[\text{Mg}/\text{Mn}]$ – $[\text{Al}/\text{Fe}]$, where the dashed line represent the limit between accreted and in-situ regions; (c) Toomre diagram, $\sqrt{V_R^2 + V_Z^2}$ versus V_ϕ . The vertical dashed line is $V_\phi = 100 \text{ km s}^{-1}$. The innermost curve represents $\|v - v_{\text{circ}}\| = 130 \text{ km s}^{-1}$ and the outermost curve is $\|v - v_{\text{circ}}\| = 220 \text{ km s}^{-1}$; (d) V_ϕ – $[\text{Fe}/\text{H}]$ space, where the horizontal dashed line is $V_\phi = 100 \text{ km s}^{-1}$; (e) Z_{max} –Eccentricity and (f) Z_{GC} – R_{GC} . The horizontal dashed line represents the Galactic plane ($Z_{\text{GC}} = 0 \text{ kpc}$), and the red star indicates the position of the Sun. In all panels, the gray points are the APOGEE sample, and the gray contours indicate the density of the low- α region. The difference between light green points and green points with a black border is only the range of metallicity of the stars.

refer to [Amarante et al. \(2022\)](#) for a detailed description of the subgrid physics and initial conditions setup.

Here, we consider models with and without a merger. For both cases, we also vary the supernova feedback², which regulates the clump formation in the first Gyr. This results in four models: *Isolated nonClumpy*, *Isolated Clumpy*, *nonClumpy+merger*, *Clumpy+merger*, and they were introduced in [Amarante et al. \(2025\)](#) as *nc.iso*, *c.iso*, *nc.r.c03*, and *c.r.c03*, respectively. Below, we describe the main properties of these models (see [Amarante et al. 2025](#) for more details).

² Either 20% or 80% of the 10^{51} erg injected per supernova, the former allowing clump formation.

In the merger models, the satellite’s orbit circularity³ is set to $\eta = 0.3$, and has a total dark matter and initial gas mass of $8.83 \times 10^{10} M_\odot$ and $1.4 \times 10^9 M_\odot$, respectively. The orbital evolution of the satellite is identical in both models; there are two clear apocentric passages with the first pericenter being at $t \approx 1.6$ Gyr, and the satellite is fully disrupted at $t \approx 3.2$ Gyr. At the first pericentric passage, the stellar mass of the satellite in the *nonClumpy+merger* and *Clumpy+merger* model is $3.15 \times 10^8 M_\odot$ and $8.97 \times 10^8 M_\odot$, respectively. These stellar masses are well within the estimated GSE stellar mass (see [Limberg et al. 2022](#) for a discussion).

The star-forming clumps in the models *Isolated Clumpy* and *Clumpy+merger* have a typical mass rang-

³ Defined as $\eta = L_z/L_c(E)$, where L_z is the satellite’s initial angular momentum, and $L_c(E)$ is the angular momentum of a planar circular orbit of energy E .

ing from $0.3 - 1 \times 10^8 M_\odot$, and they typically survive for $\approx 35 - 300$ Myr (Garver et al. 2023), in agreement with values measured from clumpy galaxies observed at redshift $z \approx 1 - 2$ (e.g. Claeysens et al. 2023). The clumps contribute up to 10-20% of the total stellar mass of the disk in the first 0.5 Gyr, and afterwards, they contribute less than 5% and cease to exist at ≈ 3 Gyr (see Figure 1 of Amarante et al. 2025). All the models are run for 10 Gyr, and we use the last snapshot to represent the “present day”. All models show a clear chemical α -bimodality in the disk, except for the *Isolated nonClumpy* model (Amarante et al. 2025).

3. RESULTS

3.1. The observed Low- α Splash population

To identify the low- α Splash members in APOGEE data, we select low- and high- α disks using $[\text{Mg}/\text{Fe}]$ – $[\text{Fe}/\text{H}]$ (Figure 1, top-left) for stars with $[\text{Fe}/\text{H}] > -1.0$. Stars above (below) the black dashed line are classified as high- α (low- α). We remove stars in the upper-left region of $[\text{Mg}/\text{Mn}]$ – $[\text{Al}/\text{Fe}]$ plane, associated with unevolved or accreted populations (Hawkins et al. 2015a; Horta et al. 2021), exclude cluster/dwarf galaxy members ($\text{MEMBERFLAG} == 0$), and restrict to $R_{\text{GC}} > 5$ kpc to avoid inner Galactic regions, resulting in 68,734 low- α and 25,676 high- α giant stars.

To define the Splash, we select stars with halo-like azimuthal velocities, $V_\phi < 100 \text{ km s}^{-1}$, consistent with Belokurov et al. (2020). By fitting a Gaussian to both low- and high- α distributions (Figure 2), we find that Splash stars correspond to the tail of the canonical disk distributions. For the high- α sample, our adopted cutoff appears to include some stars belonging to the expected high- α disk distribution. For instance, Amarante et al. (2020b) found that $\sim 13\%$ of thick-disk stars have halo-like kinematics. In this work, all stars below the threshold are classified as Splash, yielding 169 low- α and 2095 high- α Splash stars. These represent a small fraction of each disk population (Figure 2, bottom). It is worth noting that stars with thin-disk chemistry and thick-disk kinematics ($100 \lesssim V_\phi (\text{km s}^{-1}) \lesssim 130$) may also be present and could have been affected by the same mechanism that gave rise to the Splash population. Although such stars can be identified in our APOGEE sample, we do not include them in our analysis in order to preserve a cleaner association between the Splash and a halo-like population.

Figure 1 shows the chemical and dynamical distributions of low- α (green) and high- α (orange) Splash stars. We highlight low- α Splash stars with $[\text{Fe}/\text{H}] > -0.6$, by including a black border in their scatter points, which are less likely to be contaminated by accreted populations. Gray contours indicate the canonical low- α disk for comparison. In the Toomre diagram ($\sqrt{V_R^2 + V_Z^2}$ versus V_ϕ , top-right panel in Figure 1), the low- α Splash is distributed across the halo region, distinct from the canonical thin disk ($V_\phi \geq 200 \text{ km s}^{-1}$). Despite exhibit-

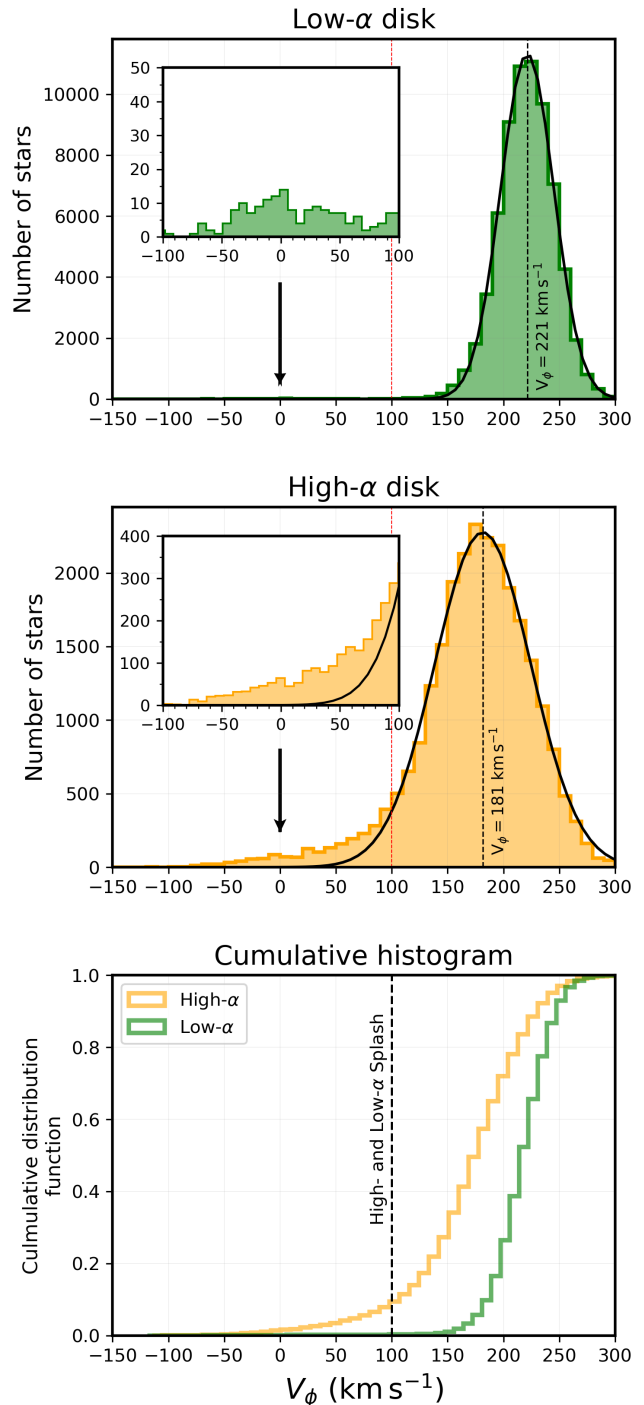


Figure 2. Distribution of azimuthal velocity V_ϕ for the low- and high- α samples in the upper and middle panels, respectively. The inner panels show a zoom on the left tail region of each distribution. The bottom panel shows the cumulative distribution of V_ϕ for both samples. The dashed vertical line at $V_\phi = 100 \text{ km s}^{-1}$ indicates the cutoff used to select the Splash population. For the Gaussian fit, we found a mean of $\langle V_\phi \rangle = 221 \text{ km s}^{-1}$ and a standard deviation of $\sigma_{V_\phi} = 24 \text{ km s}^{-1}$ for the low- α disk, while for the high- α sample, the values are $\langle V_\phi \rangle = 181 \text{ km s}^{-1}$ and $\sigma_{V_\phi} = 43 \text{ km s}^{-1}$.

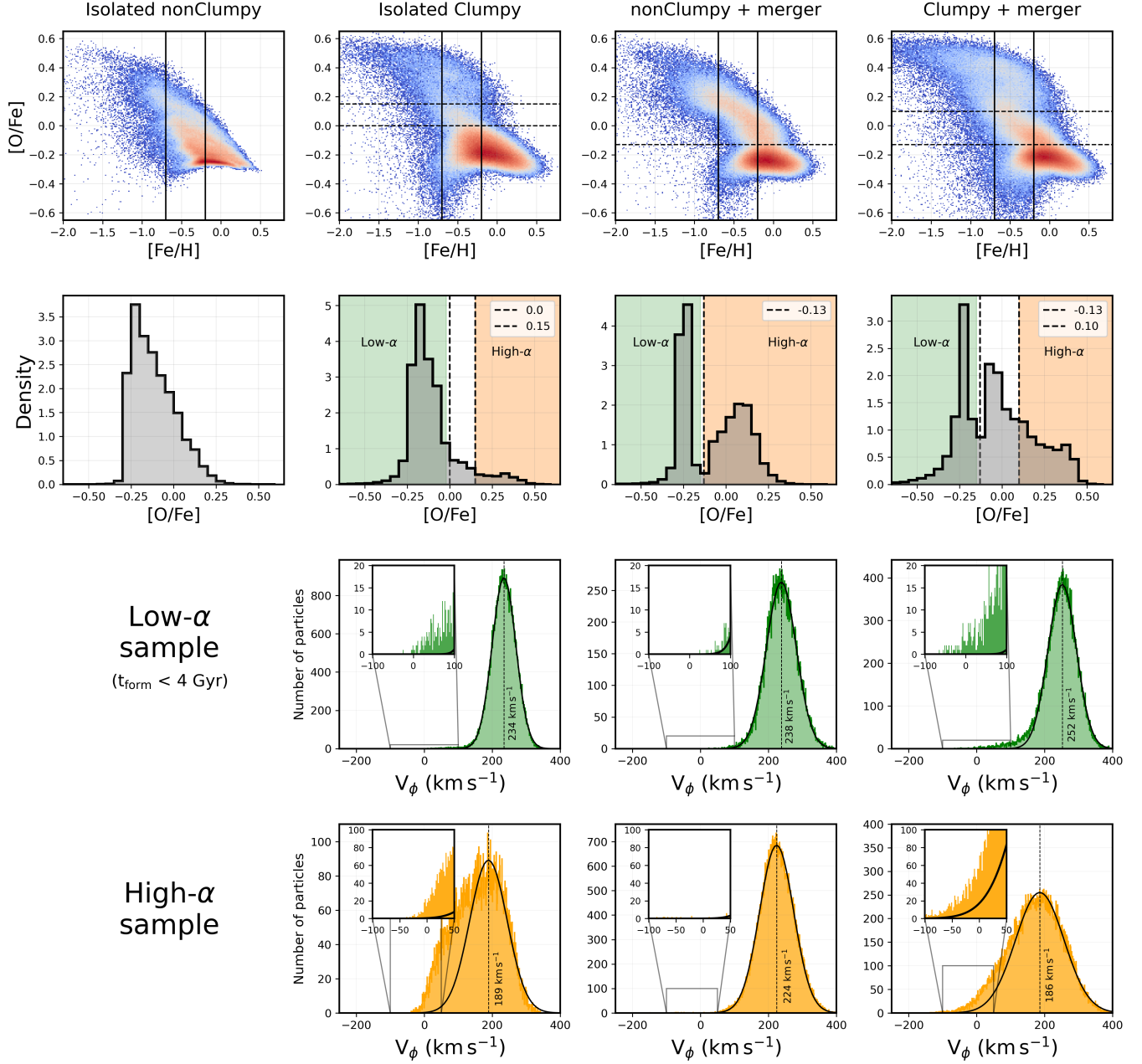


Figure 3. From left to right, the columns show the **Isolated nonClumpy**, **Isolated Clumpy**, **nonClumpy+merger**, and **Clumpy+merger** simulations. **First row:** projection onto the $[\text{O}/\text{Fe}]$ – $[\text{Fe}/\text{H}]$ plane, where red colors indicate regions of highest stellar density; the vertical lines delimit the interval $-0.7 < [\text{Fe}/\text{H}] < -0.2$, and the dashed horizontal line marks the cutoff separating the high- and low- α populations. **Second row:** $[\text{O}/\text{Fe}]$ distributions within $-0.7 < [\text{Fe}/\text{H}] < -0.2$ for each simulation; the dashed vertical lines indicate the high- and low- α separation. **Third row:** V_ϕ distributions for the low- α population (Age > 6 Gyr) in the three simulations that form a bimodality. The inset panels show a zoom of the highlighted region ($V_\phi < 100 \text{ km s}^{-1}$), and the dashed vertical line indicates the $\langle V_\phi \rangle$ of each Gaussian fit. **Fourth row:** same as the third row, but for the high- α population and highlighted region ($V_\phi < 50 \text{ km s}^{-1}$).

ing chemical compositions characteristic of the thin disk, these stars display higher orbital eccentricities and extend to vertical heights ($|Z_{\text{GC}}|$) significantly above the thin disk scale height of $h_z = 0.3 \text{ kpc}$ (Jurić et al. 2008). Note that almost all the stars in both parts of the Splash

have $e > 0.6$, which is consistent with Kisku et al. (2025) definition for Splash selection based on an eccentricity cutoff.

The kinematic similarity between the low- and high- α Splash suggests a common dynamical origin. The high- α

Splash population is thought to have formed as a consequence of the GSE merger with the pre-existing disk (Bonaca et al. 2020; Belokurov et al. 2020; Lee et al. 2023) or through an early clumpy formation phase at $z \sim 1 - 2$ (Amarante et al. 2020a). Thus, if the formation of both Splash populations are related, it requires the presence of an ancient low- α /thin disk population as described in Borbolato et al. (2025).

3.2. Low- α Splash in simulated MW analog galaxy

Amarante et al. (2020a) analysed the formation of the high- α Splash using two isolated models, the **Isolated nonClumpy** and **Isolated Clumpy**⁴. Here, we extend this framework by including two MW analogs undergoing a GSE-like merger, with (**Clumpy+merger**) and without (**nonClumpy+merger**) massive star-forming clumps.

Figure 3 shows the properties of the simulated stellar populations. To better reproduce the same Galactic region used in the observational data, we normalized the disk length by the scale length of each simulation, whose exact values can be found in Table 1 of Amarante et al. (2025). Only the **Isolated nonClumpy** model fails to develop the $[\text{O}/\text{Fe}]$ – $[\text{Fe}/\text{H}]$ ⁵ bimodality characteristic of the MW (first row of Figure 3). Consequently, we focus on the three bimodal models, separating high- and low- α populations using the $[\text{O}/\text{Fe}]$ distribution (second row panels). Note that for the clumpy models, we introduced a gap between the two populations to avoid regions where they may overlap. Following the observational procedure described in Subsection 2.1, low- α Splash stars are defined by $V_\phi < 100 \text{ km s}^{-1}$, while a stricter cut ($V_\phi < 50 \text{ km s}^{-1}$) is adopted for high- α stars. Since the high- α population is more dynamically heated in the simulations compared to the MW, this more restrictive cutoff helps reduce contamination from the canonical disk distribution. Crucially, only clumpy models produce an extended V_ϕ tail for both high- and low- α populations. The **nonClumpy+merger** simulation does not produce a Splash component, contradicting the expectations that a GSE-like merger alone would produce the α -rich Splash (see Section 4). We note that the stellar mass of the GSE-like galaxy in this model is at the lower end of the measured values (Lane et al. 2023). For the low- α disk, we choose to project only old stars ($t_{\text{form}}^6 < 4 \text{ Gyr}$) in Figure 3 to show the low- V_ϕ tail of canonical thin disk distribution (see Figure 3 of Borbolato et al. 2025 for observational evidence that the old low- α disk displays a larger velocity dispersion than its younger counterpart), but no age cut is applied to

⁴ Their clumpy phase is more intense than in our models

⁵ In the simulations, Oxygen is the tracer of the α -element.

⁶ The parameter t_{form} corresponds to the time at which a star forms in the simulation, where $t_{\text{form}} = 0 \text{ Gyr}$ marks the beginning of the simulation and $t_{\text{form}} = 10 \text{ Gyr}$ its end, representing the present day

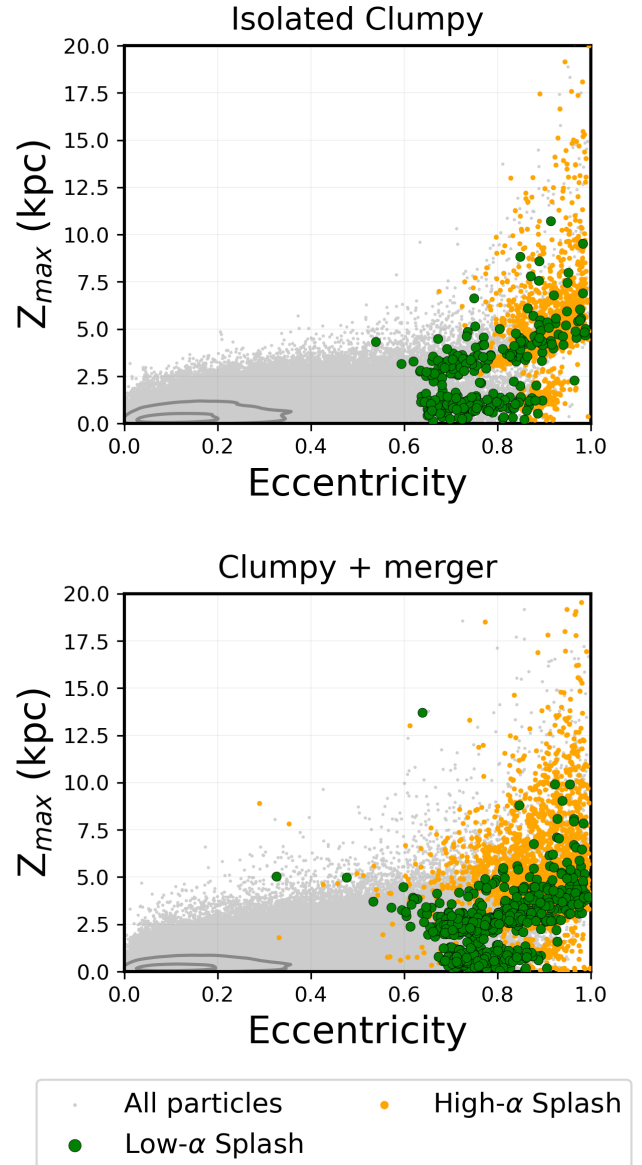


Figure 4. Distribution of high- and low- α Splash populations on the Z_{max} vs. eccentricity space for the **Isolated Clumpy** (top) and the **Clumpy+merger** (bottom panel) models. Gray points represent all particles in the simulation, and the gray contours indicates the higher-density region of the low- α /thin disk. The high- α Splash is shown in orange points, while the low- α Splash is the green ones.

the full sample. We projected the selected Splash populations onto the Z_{max} –Eccentricity space in Figure 4, reproducing panel (e) of Figure 1. Similarly to the observational data, the $V_\phi < 100 \text{ km s}^{-1}$ selection in the simulations is effective at isolating stars on halo-like orbits (high eccentricity, $e > 0.6$), i.e. Splash stars. We note that the apparent wedges in the Z_{max} –Eccentricity plane, also seen in the observational data, is a dynamical

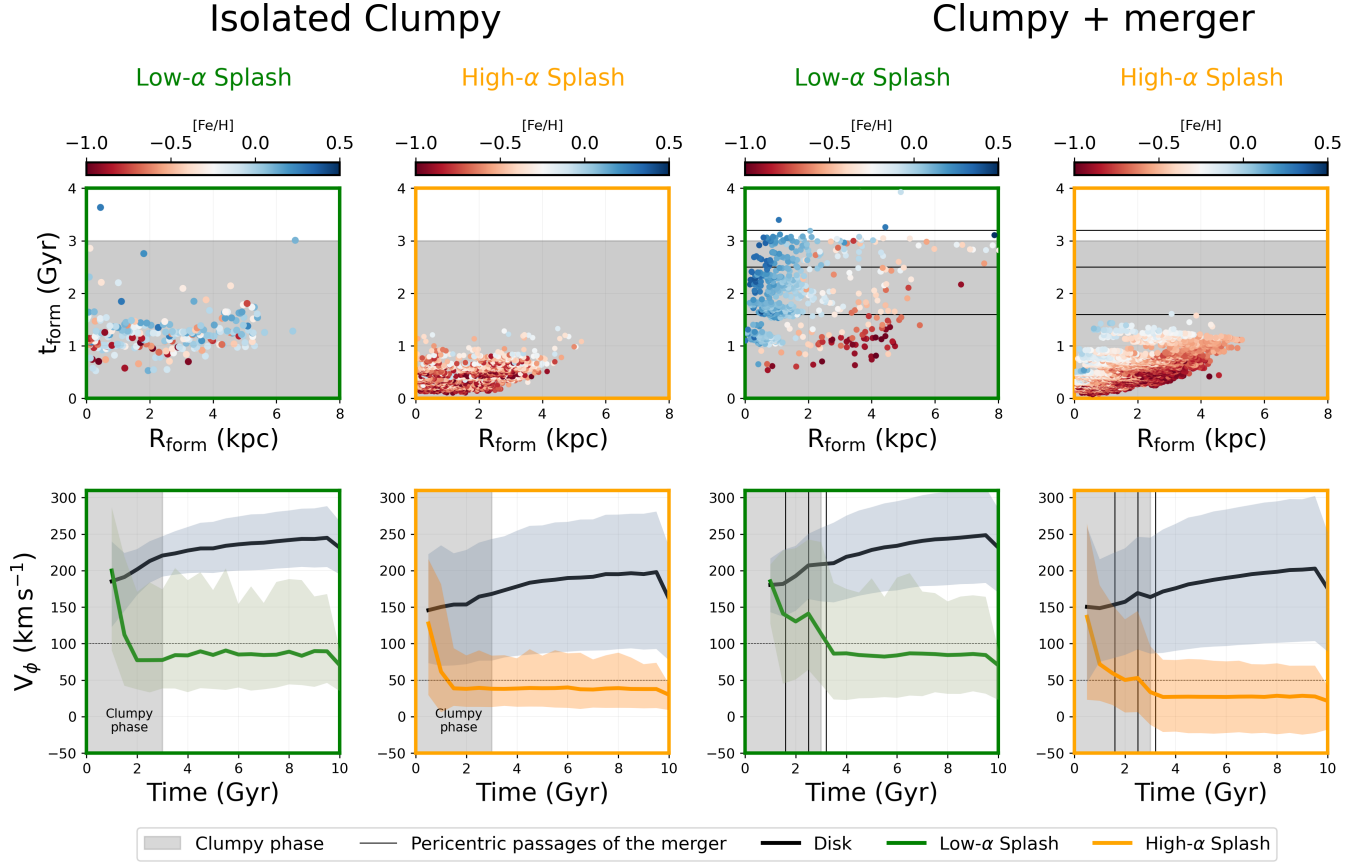


Figure 5. The first two columns show the **Isolated Clumpy** model, while the last two columns show the **Clumpy+Merger** model. **Top row:** distribution of low- and high- α Splash stars in the $t_{\text{form}}-R_{\text{form}}$ plane, colored by $[\text{Fe}/\text{H}]$, being the t_{form} the star formation time and R_{form} the galactocentric radius at which each star formed. The horizontal lines in the two panels on the right indicate $t_{\text{form}} = 1.6, 2.5,$ and 3.2 Gyr, corresponding to the first, second, and final pericentric passages of the dwarf galaxy, respectively. **Bottom row:** evolution of V_ϕ as a function of time for the low- and high- α Splash populations. The Splash populations are represented by the colored lines, while the canonical low- and high- α disks are shown by the upper black line. The vertical lines mark the same pericentric passages of the dwarf galaxy indicated in the top panels. The gray band in all panels indicates the period of the clumpy phase (first 3 Gyr).

cal effect which depends on the potential of the galaxy (Amarante et al. 2020b; Koppelman et al. 2021).

Figure 5 explores Splash formation in the **Isolated Clumpy** and **Clumpy+merger** models. The top panels show formation radius, R_{form} , and time of formation, t_{form} , colored by $[\text{Fe}/\text{H}]$. Splash stars in both models form primarily during the first 3 Gyr, coinciding with the clumpy phase. In the **Clumpy+merger** case, pericentric passages of the dwarf galaxy are marked at $t = 1.6, 2.5,$ and 3.2 Gyr. Although stars at $R_{\text{GC}} < 5$ kpc are excluded from the analysis, most Splash stars originate in the inner Galaxy. Other notable feature is that while the **Isolated Clumpy** model does not have a $[\text{Fe}/\text{H}]$ gradient with R_{form} , the **Clumpy+merger** model has a radial metallicity gradient at a given t_{form} . The formation of metallicity gradients in clumpy and non-clumpy MW models merits its own separate investigation.

The evolution of the mean V_ϕ (bottom panels of Figure 5) shows that, while the disk remains rotationally

supported, Splash stars are rapidly heated in all the clumpy models, with or without mergers, indicating that clumps dominate the process. For the **Clumpy+merger** model, we observe a peak in the mean V_ϕ immediately following the second pericentric passage of the dwarf. The decline in V_ϕ at 10 Gyr, in both models, is a selection artifact due to the criteria used to define Splash stars. We verify that this drop in median V_ϕ also occurs when the selection is made at previous snapshots.

4. DISCUSSION

Borbolato et al. (2025) presented observational evidence for the co-formation of the thick/high- α and thin/low- α disks using precise stellar ages from the isochrone-fitting **StarHorse** code (Queiroz et al. 2023). In particular, they found that the thin disk was already in place before the GSE dwarf merger, reinforcing previous studies indicating an early thin disk formation (e.g., Silva Aguirre et al. 2018; Beraldo e Silva et al. 2021;

Nepal et al. 2024; Gent et al. 2024). The presence of a low- α Splash component therefore supports a pre-GSE old thin disk, independent of age estimates. The idea that the Splash population may also include low- α stars was shown in Nepal et al. (2024), based on observational data from Gaia DR3 Radial Velocity Spectrometer (RVS) spectra (Cropper et al. 2018), chemical abundances ($[\alpha/\text{Fe}]$ and $[\text{Fe}/\text{H}]$) derived using a hybrid convolutional neural network method (Guiglion et al. 2024) and ages from the *StarHorse* code. They showed that the region traditionally associated with the Splash in the V_ϕ - $[\text{Fe}/\text{H}]$ diagram is also populated by low- α stars older than 9 Gyr. However, they did not investigate the mechanisms responsible for the formation of this population and its clear association with the high- α Splash. Some low- α Splash stars are also visible in Kisku et al. (2025) (see their figure 6), although they are not discussed.

The kinematic similarity between the low- and high- α Splash in our analysis suggests a common dynamical heating mechanism, which is attributed to scattering by massive, early star-forming clumps (similar to Amarante et al. 2020a), a process that simultaneously affects both chemical populations. Clumpy models are uniquely able to reproduce both the Splash population and the old (Age > 10 Gyr) low- α disk. Our results provide a counterpoint to recent literature on the origin of low- α metal-rich halo stars. While Lee et al. (2023) attributed this population up to $[\text{Fe}/\text{H}] < -0.6$ to GSE accretion, this does not explain the low- α Splash stars we observe at $\text{Fe}/\text{H} > -0.6$. While the low-metallicity regime may include contamination from dwarf galaxies such as the GSE (e.g., Feuillet et al. 2020; Naidu et al. 2021; Limberg et al. 2022), no known major merger reaches $[\text{Fe}/\text{H}] > -0.6$, implying an in-situ origin. Furthermore, the $[\text{Fe}/\text{H}]$ range of the low- α Splash is consistent with that of the old thin disk (e.g., Silva Aguirre et al. 2018; Nepal et al. 2024; Borbolato et al. 2025). Note that the low- α stars of solar and supersolar metallicity dating from the first billion years in the *Clumpy+merger* model are born in the central region of the Galaxy, where faster chemical enrichment is expected since early stages (see Figure 5).

Alternative formation scenarios for the Splash have been proposed, including minor mergers or bar resonances. While some models propose that multiple retrograde minor mergers could form the Splash (e.g. Kisku et al. 2025), the observed preference for prograde minor mergers in the MW makes this unlikely (Malhan et al. 2022). Likewise, the Galactic bar is unlikely to explain retrograde stars in the solar neighborhood. Fiteni et al. (2021) showed that bar-driven retrograde stars remain near the bar vicinity, while retrograde stars in the solar neighborhood, in clumpy models, are exclusively clump-driven. Finally, we note a discrepancy with some cosmological simulations that favor a major-merger origin for the Splash (e.g. Grand et al. 2020; Liao et al. 2024;

Orkney & Laporte 2025). We argue that although the GASTRO simulations are more tailored-made experiments, with a controlled merger configuration that reproduces the GSE dwarf merger (Amarante et al. 2022), it still provides an accurate representation of the the formation history of the MW's disk (Amarante et al. 2025).

Our findings align with Amarante et al. (2020a), who demonstrated that the high- α Splash arises from clump scattering in the early disk, and with Buder et al. (2025), who link the Splash to the dispersion-dominated nature of the proto-galaxy. In the latter case, extragalactic studies similarly showed that massive clumps strongly affect velocity fields and enhance the disk velocity dispersion (e.g., Erb et al. 2004; Weiner et al. 2006), contributing to the dispersion-dominated nature of early disks.

5. CONCLUSIONS

This Letter has investigated the existence of a low- α Splash in the MW. For this goal, we use spectroscopic data of red giant stars from APOGEE DR17 with distances from *StarHorse* and astrometry from *Gaia* DR3. Furthermore, we investigated the Splash formation (low- and high- α) using GASTRO suite simulation focused on reproducing the main characteristics of the MW. We consider two main paths for the formation of such a population: the dynamical heating by scattering clumps or by the MW's last major merger with the GSE disrupted dwarf galaxy. Our main conclusions are summarized as follows:

- (i) We report the existence of stars chemically compatible with the low- α /thin disk on halo-like orbits in the APOGEE sample of red giant stars, and dub this population as low- α Splash.
- (ii) We argue that the low- α Splash was formed by the same mechanism that gave rise to the traditional high- α Splash, implying that an old low- α /thin disk must have already existed since the first billion years of the MW. This ancient thin disk population has been discussed in previous works with stellar ages. However, the low- α Splash constitutes observational evidence that is independent of these age estimates.
- (iii) We show that the high- and low- α Splash are likely formed by the scattering of clumps in an isolated simulation, without the need for the merger. This result is compatible with the proposals of Amarante et al. (2020a) and Buder et al. (2025), and also aligns with the need for the presence of clumps during the formation of the proto-disk, required to produce old low- α stars by the clumpy model.
- (iv) A GSE-like merger in an MW-analog galaxy does not significantly heat the disk to create a Splash-like population.

The Splash population, now separated into high- α and low- α components, remains important in investigating the early phases of the MW, as they are associated with the Galactic proto-disk. Detailed analysis of these populations can reveal important insights into the mechanisms that governed the disk’s evolution at that time.

ACKNOWLEDGMENTS

L.B. thanks the partial financial support by the São Paulo Research Foundation (FAPESP), Brasil (Proc. 2024/16510-2), CAPES/PROEX (proc. 88887.821814/2023-00), and also thanks to all those involved with the multi-institutional *Milky Way BR* Group for the weekly discussions. JA and ZYL are supported by the National Natural Science Foundation of China under grant No. 12233001, by the National Key R&D Program of China under grant No. 2024YFA1611602, by a Shanghai Natural Science Research Grant (24ZR1491200), by the “111” project of the Ministry of Education under grant No. B20019, and by the China Manned Space Project with No. CMS-CSST-2021-B03. JA and ZYL also thank the sponsorship from Yangyang Development Fund. S.R. also thanks partial financial support from FAPESP (Proc. 2020/15245-2), CNPq (Proc. 303816/2022-8), and CAPES. TK acknowledges support from the NSFC (Grant No. 12303013) and support from the China Postdoctoral Science Foundation (Grant No. 2023M732250).

This work has made use of data from the European Space Agency (ESA) mission *Gaia* (<https://www.cosmos.esa.int/gaia>), processed by the *Gaia* Data Processing and Analysis Consortium (DPAC, <https://www.cosmos.esa.int/web/gaia/dpac/consortium>). Funding for the DPAC has been provided by national institutions, in particular, the institutions participating in the *Gaia* Multilateral Agreement.

REFERENCES

- Abdurro'uf, Accetta, K., Aerts, C., et al. 2022, *ApJS*, 259, 35, doi: [10.3847/1538-4365/ac4414](https://doi.org/10.3847/1538-4365/ac4414)
- Adams, D., Dickinson, H., Fortson, L., et al. 2025, *ApJ*, 979, 118, doi: [10.3847/1538-4357/ad7119](https://doi.org/10.3847/1538-4357/ad7119)
- Agertz, O., Renaud, F., Feltzing, S., et al. 2021, *MNRAS*, 503, 5826, doi: [10.1093/mnras/stab322](https://doi.org/10.1093/mnras/stab322)
- Amarante, J. A. S., Beraldo e Silva, L., Debattista, V. P., & Smith, M. C. 2020a, *ApJL*, 891, L30, doi: [10.3847/2041-8213/ab78a4](https://doi.org/10.3847/2041-8213/ab78a4)
- Amarante, J. A. S., Debattista, V. P., Beraldo e Silva, L., Laporte, C. F. P., & Deg, N. 2022, *ApJ*, 937, 12, doi: [10.3847/1538-4357/ac8b0d](https://doi.org/10.3847/1538-4357/ac8b0d)
- Amarante, J. A. S., Smith, M. C., & Boeche, C. 2020b, *MNRAS*, 492, 3816, doi: [10.1093/mnras/staa077](https://doi.org/10.1093/mnras/staa077)
- Amarante, J. A. S., Laporte, C. F. P., Debattista, V. P., et al. 2025, arXiv e-prints, arXiv:2512.01293, doi: [10.48550/arXiv.2512.01293](https://doi.org/10.48550/arXiv.2512.01293)
- Barbuy, B., Chiappini, C., & Gerhard, O. 2018, *ARA&A*, 56, 223, doi: [10.1146/annurev-astro-081817-051826](https://doi.org/10.1146/annurev-astro-081817-051826)
- Belokurov, V., Erkal, D., Evans, N. W., Koposov, S. E., & Deason, A. J. 2018, *MNRAS*, 478, 611, doi: [10.1093/mnras/sty982](https://doi.org/10.1093/mnras/sty982)
- Belokurov, V., Sanders, J. L., Fattahi, A., et al. 2020, *MNRAS*, 494, 3880, doi: [10.1093/mnras/staa876](https://doi.org/10.1093/mnras/staa876)
- Beraldo e Silva, L., Debattista, V. P., Khachatryan, T., & Nidever, D. 2020, *MNRAS*, 492, 4716, doi: [10.1093/mnras/staa065](https://doi.org/10.1093/mnras/staa065)
- Beraldo e Silva, L., Debattista, V. P., Nidever, D., Amarante, J. A. S., & Garver, B. 2021, *MNRAS*, 502, 260, doi: [10.1093/mnras/staa3966](https://doi.org/10.1093/mnras/staa3966)
- Bland-Hawthorn, J., & Gerhard, O. 2016, *ARA&A*, 54, 529, doi: [10.1146/annurev-astro-081915-023441](https://doi.org/10.1146/annurev-astro-081915-023441)
- Bonaca, A., Conroy, C., Wetzell, A., Hopkins, P. F., & Kereš, D. 2017, *ApJ*, 845, 101, doi: [10.3847/1538-4357/aa7d0c](https://doi.org/10.3847/1538-4357/aa7d0c)
- Bonaca, A., Conroy, C., Cargile, P. A., et al. 2020, *ApJL*, 897, L18, doi: [10.3847/2041-8213/ab9caa](https://doi.org/10.3847/2041-8213/ab9caa)
- Borbolato, L., Rossi, S., Perottoni, H. D., et al. 2025, *ApJ*, 994, 126, doi: [10.3847/1538-4357/ae0c96](https://doi.org/10.3847/1538-4357/ae0c96)
- Bournaud, F., Daddi, E., Elmegreen, B. G., et al. 2008, *A&A*, 486, 741, doi: [10.1051/0004-6361:20079250](https://doi.org/10.1051/0004-6361:20079250)
- Buder, S., Buck, T., Skúladóttir, Á., et al. 2025, arXiv e-prints, arXiv:2510.20233, doi: [10.48550/arXiv.2510.20233](https://doi.org/10.48550/arXiv.2510.20233)
- Chiappini, C., Matteucci, F., & Gratton, R. 1997, *ApJ*, 477, 765, doi: [10.1086/303726](https://doi.org/10.1086/303726)
- Claeyssens, A., Adamo, A., Richard, J., et al. 2023, *MNRAS*, 520, 2180, doi: [10.1093/mnras/stac3791](https://doi.org/10.1093/mnras/stac3791)
- Clarke, A. J., Debattista, V. P., Nidever, D. L., et al. 2019, *MNRAS*, 484, 3476, doi: [10.1093/mnras/stz104](https://doi.org/10.1093/mnras/stz104)
- Cropper, M., Katz, D., Sartoretti, P., et al. 2018, *A&A*, 616, A5, doi: [10.1051/0004-6361/201832763](https://doi.org/10.1051/0004-6361/201832763)
- da Silva, A. R., & Smiljanic, R. 2025, *A&A*, 696, A122, doi: [10.1051/0004-6361/202453295](https://doi.org/10.1051/0004-6361/202453295)
- de la Vega, A., Mobasher, B., Sattari, Z., et al. 2025, arXiv e-prints, arXiv:2508.14972, doi: [10.48550/arXiv.2508.14972](https://doi.org/10.48550/arXiv.2508.14972)
- Debattista, V. P., Liddicott, D. J., Gonzalez, O. A., et al. 2023, *ApJ*, 946, 118, doi: [10.3847/1538-4357/acbb00](https://doi.org/10.3847/1538-4357/acbb00)
- Di Matteo, P., Haywood, M., Lehnert, M. D., et al. 2019, *A&A*, 632, A4, doi: [10.1051/0004-6361/201834929](https://doi.org/10.1051/0004-6361/201834929)
- Dillamore, A. M., Belokurov, V., Font, A. S., & McCarthy, I. G. 2022, *MNRAS*, 513, 1867, doi: [10.1093/mnras/stac1038](https://doi.org/10.1093/mnras/stac1038)
- Erb, D. K., Steidel, C. C., Shapley, A. E., Pettini, M., & Adelberger, K. L. 2004, *ApJ*, 612, 122, doi: [10.1086/422464](https://doi.org/10.1086/422464)
- Feuillet, D. K., Feltzing, S., Sahlholdt, C. L., & Casagrande, L. 2020, *MNRAS*, 497, 109, doi: [10.1093/mnras/staa1888](https://doi.org/10.1093/mnras/staa1888)
- Filion, C., Petersen, M. S., Horta, D., et al. 2025, *ApJ*, 989, 70, doi: [10.3847/1538-4357/ade2d2](https://doi.org/10.3847/1538-4357/ade2d2)
- Fiteni, K., Caruana, J., Amarante, J. A. S., Debattista, V. P., & Beraldo e Silva, L. 2021, *MNRAS*, 503, 1418, doi: [10.1093/mnras/stab619](https://doi.org/10.1093/mnras/stab619)
- Freeman, K., & Bland-Hawthorn, J. 2002, *ARA&A*, 40, 487, doi: [10.1146/annurev.astro.40.060401.093840](https://doi.org/10.1146/annurev.astro.40.060401.093840)
- Gaia Collaboration, Prusti, T., de Bruijne, J. H. J., et al. 2016, *A&A*, 595, A1, doi: [10.1051/0004-6361/201629272](https://doi.org/10.1051/0004-6361/201629272)
- Gaia Collaboration, Vallenari, A., Brown, A. G. A., et al. 2023, *A&A*, 674, A1, doi: [10.1051/0004-6361/202243940](https://doi.org/10.1051/0004-6361/202243940)
- Gallart, C., Bernard, E. J., Brook, C. B., et al. 2019, *Nature Astronomy*, 3, 932, doi: [10.1038/s41550-019-0829-5](https://doi.org/10.1038/s41550-019-0829-5)
- Garver, B. R., Nidever, D. L., Debattista, V. P., Beraldo e Silva, L., & Khachatryan, T. 2023, *ApJ*, 953, 128, doi: [10.3847/1538-4357/acdfc6](https://doi.org/10.3847/1538-4357/acdfc6)
- Gent, M. R., Eitner, P., Serenelli, A., et al. 2024, *A&A*, 683, A74, doi: [10.1051/0004-6361/202244157](https://doi.org/10.1051/0004-6361/202244157)
- Grand, R. J. J., Kawata, D., Belokurov, V., et al. 2020, *MNRAS*, 497, 1603, doi: [10.1093/mnras/staa2057](https://doi.org/10.1093/mnras/staa2057)
- Grisoni, V., Spitoni, E., & Matteucci, F. 2026, arXiv e-prints, arXiv:2605.10596, doi: [10.48550/arXiv.2605.10596](https://doi.org/10.48550/arXiv.2605.10596)
- Grisoni, V., Spitoni, E., Matteucci, F., et al. 2017, *MNRAS*, 472, 3637, doi: [10.1093/mnras/stx2201](https://doi.org/10.1093/mnras/stx2201)
- Guiglion, G., Nepal, S., Chiappini, C., et al. 2024, *A&A*, 682, A9, doi: [10.1051/0004-6361/202347122](https://doi.org/10.1051/0004-6361/202347122)

- Guo, Y., Ferguson, H. C., Bell, E. F., et al. 2015, *ApJ*, 800, 39, doi: [10.1088/0004-637X/800/1/39](https://doi.org/10.1088/0004-637X/800/1/39)
- Hawkins, K., Jofré, P., Masseron, T., & Gilmore, G. 2015a, *MNRAS*, 453, 758, doi: [10.1093/mnras/stv1586](https://doi.org/10.1093/mnras/stv1586)
- Hawkins, K., Kordopatis, G., Gilmore, G., et al. 2015b, *MNRAS*, 447, 2046, doi: [10.1093/mnras/stu2574](https://doi.org/10.1093/mnras/stu2574)
- Haywood, M., Di Matteo, P., Lehnert, M. D., et al. 2018, *ApJ*, 863, 113, doi: [10.3847/1538-4357/aad235](https://doi.org/10.3847/1538-4357/aad235)
- Helmi, A. 2020, *ARA&A*, 58, 205, doi: [10.1146/annurev-astro-032620-021917](https://doi.org/10.1146/annurev-astro-032620-021917)
- Helmi, A., Babusiaux, C., Koppelman, H. H., et al. 2018, *Nature*, 563, 85, doi: [10.1038/s41586-018-0625-x](https://doi.org/10.1038/s41586-018-0625-x)
- Horta, D., Schiavon, R. P., Mackereth, J. T., et al. 2021, *MNRAS*, 500, 1385, doi: [10.1093/mnras/staa2987](https://doi.org/10.1093/mnras/staa2987)
- Imig, J., Price, C., Holtzman, J. A., et al. 2023, *ApJ*, 954, 124, doi: [10.3847/1538-4357/ace9b8](https://doi.org/10.3847/1538-4357/ace9b8)
- Jönsson, H., Holtzman, J. A., Allende Prieto, C., et al. 2020, *AJ*, 160, 120, doi: [10.3847/1538-3881/aba592](https://doi.org/10.3847/1538-3881/aba592)
- Jurić, M., Ivezić, Ž., Brooks, A., et al. 2008, *ApJ*, 673, 864, doi: [10.1086/523619](https://doi.org/10.1086/523619)
- Kisku, S., Schiavon, R. P., Font, A. S., et al. 2025, *MNRAS*, 542, 76, doi: [10.1093/mnras/staf1075](https://doi.org/10.1093/mnras/staf1075)
- Koppelman, H. H., Hagen, J. H. J., & Helmi, A. 2021, *A&A*, 647, A37, doi: [10.1051/0004-6361/202039390](https://doi.org/10.1051/0004-6361/202039390)
- Lane, J. M. M., Bovy, J., & Mackereth, J. T. 2023, *MNRAS*, 526, 1209, doi: [10.1093/mnras/stad2834](https://doi.org/10.1093/mnras/stad2834)
- Lee, A., Lee, Y. S., Kim, Y. K., Beers, T. C., & An, D. 2023, *ApJ*, 945, 56, doi: [10.3847/1538-4357/acb6f5](https://doi.org/10.3847/1538-4357/acb6f5)
- Liao, X., Li, Z.-Y., Simion, I., et al. 2024, *ApJ*, 967, 5, doi: [10.3847/1538-4357/ad38ba](https://doi.org/10.3847/1538-4357/ad38ba)
- Limberg, G., Souza, S. O., Pérez-Villegas, A., et al. 2022, *ApJ*, 935, 109, doi: [10.3847/1538-4357/ac8159](https://doi.org/10.3847/1538-4357/ac8159)
- Lindgren, L., Klioner, S. A., Hernández, J., et al. 2021, *A&A*, 649, A2, doi: [10.1051/0004-6361/202039709](https://doi.org/10.1051/0004-6361/202039709)
- Majewski, S. R., Schiavon, R. P., Frinchaboy, P. M., et al. 2017, *AJ*, 154, 94, doi: [10.3847/1538-3881/aa784d](https://doi.org/10.3847/1538-3881/aa784d)
- Malhan, K., Ibata, R. A., Sharma, S., et al. 2022, *ApJ*, 926, 107, doi: [10.3847/1538-4357/ac4d2a](https://doi.org/10.3847/1538-4357/ac4d2a)
- McMillan, P. J. 2017, *MNRAS*, 465, 76, doi: [10.1093/mnras/stw2759](https://doi.org/10.1093/mnras/stw2759)
- Montalbán, J., Mackereth, J. T., Miglio, A., et al. 2021, *Nature Astronomy*, 5, 640, doi: [10.1038/s41550-021-01347-7](https://doi.org/10.1038/s41550-021-01347-7)
- Naidu, R. P., Conroy, C., Bonaca, A., et al. 2021, *ApJ*, 923, 92, doi: [10.3847/1538-4357/ac2d2d](https://doi.org/10.3847/1538-4357/ac2d2d)
- Nepal, S., Chiappini, C., Queiroz, A. B., et al. 2024, *A&A*, 688, A167, doi: [10.1051/0004-6361/202449445](https://doi.org/10.1051/0004-6361/202449445)
- Orkney, M. D. A., & Laporte, C. F. P. 2025, arXiv e-prints, arXiv:2509.09576, doi: [10.48550/arXiv.2509.09576](https://doi.org/10.48550/arXiv.2509.09576)
- Ortigoza-Urdaneta, M., Vieira, K., Fernández-Trincado, J. G., et al. 2023, *A&A*, 676, A140, doi: [10.1051/0004-6361/202346325](https://doi.org/10.1051/0004-6361/202346325)
- Puech, M. 2010, *MNRAS*, 406, 535, doi: [10.1111/j.1365-2966.2010.16689.x](https://doi.org/10.1111/j.1365-2966.2010.16689.x)
- Queiroz, A. B. A., Anders, F., Chiappini, C., et al. 2023, *A&A*, 673, A155, doi: [10.1051/0004-6361/202245399](https://doi.org/10.1051/0004-6361/202245399)
- Renaud, F., Agertz, O., Andersson, E. P., et al. 2021, *MNRAS*, 503, 5868, doi: [10.1093/mnras/stab543](https://doi.org/10.1093/mnras/stab543)
- Sattari, Z., Mobasher, B., Chartab, N., et al. 2023, *ApJ*, 951, 147, doi: [10.3847/1538-4357/acd5d6](https://doi.org/10.3847/1538-4357/acd5d6)
- Schönrich, R., Binney, J., & Dehnen, W. 2010, *MNRAS*, 403, 1829, doi: [10.1111/j.1365-2966.2010.16253.x](https://doi.org/10.1111/j.1365-2966.2010.16253.x)
- Sheffield, A. A., Majewski, S. R., Johnston, K. V., et al. 2012, *ApJ*, 761, 161, doi: [10.1088/0004-637X/761/2/161](https://doi.org/10.1088/0004-637X/761/2/161)
- Shibuya, T., Ouchi, M., Kubo, M., & Harikane, Y. 2016, *ApJ*, 821, 72, doi: [10.3847/0004-637X/821/2/72](https://doi.org/10.3847/0004-637X/821/2/72)
- Silva Aguirre, V., Bojsen-Hansen, M., Slumstrup, D., et al. 2018, *MNRAS*, 475, 5487, doi: [10.1093/mnras/sty150](https://doi.org/10.1093/mnras/sty150)
- Sok, V., Muzzin, A., Tan, V. Y. Y., et al. 2025, arXiv e-prints, arXiv:2509.25363, doi: [10.48550/arXiv.2509.25363](https://doi.org/10.48550/arXiv.2509.25363)
- Spitoni, E., Silva Aguirre, V., Matteucci, F., Calura, F., & Grisoni, V. 2019, *A&A*, 623, A60, doi: [10.1051/0004-6361/201834188](https://doi.org/10.1051/0004-6361/201834188)
- Tan, V. Y. Y., Muzzin, A., Sarrouh, G. T. E., et al. 2025, *ApJ*, 994, 94, doi: [10.3847/1538-4357/ae0ffe](https://doi.org/10.3847/1538-4357/ae0ffe)
- Vasiliev, E. 2019, *MNRAS*, 482, 1525, doi: [10.1093/mnras/sty2672](https://doi.org/10.1093/mnras/sty2672)
- Weiner, B. J., Willmer, C. N. A., Faber, S. M., et al. 2006, *ApJ*, 653, 1027, doi: [10.1086/508921](https://doi.org/10.1086/508921)
- Wilson, J. C., Hearty, F. R., Skrutskie, M. F., et al. 2019, *PASP*, 131, 055001, doi: [10.1088/1538-3873/ab0075](https://doi.org/10.1088/1538-3873/ab0075)
- Zanella, A., Le Floch, E., Harrison, C. M., et al. 2019, *MNRAS*, 489, 2792, doi: [10.1093/mnras/stz2099](https://doi.org/10.1093/mnras/stz2099)